Pergamon

Int. J. Solids Structures Vol. 34, Nos. 35–36, pp. 4547–4556, 1997

0020-7683/97 $17.00 + .00

PII: S0020-7683(97)00040-1

MODEL FOR 28CrMoV5-8 STEEL UNDERGOING THERMOMECHANICAL CYCLIC LOADINGS

H. SAMROUT and R. EL ABDI†
Laboratoire Génie de Production-Ecole Nationale d'Ingénieurs, B. P. 1629,
65016 Tarbes Cedex, France

and

J. L. CHABOCHE
O.N.E.R.A. Direction des Structures, B. P. 72 F-92322 Chatillon Cedex, France

(*Received* 23 *July* 1996; *in revised form* 14 *January* 1997)

Abstract—An anisothermal elastoviscoplastic three-dimensional model is proposed in order to predict the response of brake discs used in the French T.G.V. (high speed train). The brake disc is subjected simultaneously to mechanical and thermal cyclic loadings by the application of brake pads to the friction surface. This anisothermal law is based on the internal thermodynamic variables and takes into account the non-linear kinematic hardening, isotropic hardening (to describe cyclic softening) and plastic strain memory effect. Cyclic viscoplastic behavior under in-phase changes of temperature and strain is analysed by using this elaborate anisothermal model with its material constants determined from isothermal experiments. Good agreement is obtained between the predictions and experiments. © 1997 Published by Elsevier Science Ltd.

1. INTRODUCTION

The modern methods for life prediction in structures need an inelastic analysis, which leads to large computing times, especially under cyclic loading. This is the case for many structures like the brake disc of the high speed train which is submitted simultaneously to mechanical and thermal cyclic loading due to the application of the brake pads to the friction surface. This structure is machined from a cast or wrought steel. The brake pads are of an organic material. The brake pads produce a heat flux which is assumed uniform on the friction surface of the disc.

Experimental studies of the steel used in the brake disc, reveal a very complex behavior under cyclic and monotonic loading. In addition to the classical Bauschinger effect and cyclic softening, a memory effect of the plastic strain is observed. The present work uses a set of constitutive equations developed to describe as correctly as possible the main experimental results obtained under cyclic loading conditions at varying temperatures.

The constitutive equations, developed at O.N.E.R.A. (Chaboche, 1989), use a decomposition of hardening into kinematic and isotropic parts, each obeying respective differential equations. The kinematic hardening is introduced in a non-linear form. For the determination of the set of constitutive equation parameters, an optimization software developed by O.N.E.R.A. (Chaboche, 1991) was used.

2. CONSTITUTIVE EQUATIONS

The constitutive equations governing the elastoviscoplastic behavior of complex structures under thermomechanical loading, must take into account complex phenomena such as viscoplasticity, cyclic softening or hardening, relaxation and strain memory effect. These phenomena have been studied by many scientists especially in the recent years (Chaboche, 1978; Nouailhas, 1989; Kawai, 1987; Krempl, 1984; Marquis, 1987; Nouailhas, 1987; Tanaka, 1987).

† Author to whom correspondence should be addressed.

The model was proposed by Chaboche (1989) and is based on the internal stress concept using a set of internal variables. The general expression of this model is as follows.

(a) *Partition of strain*

$$\varepsilon = \varepsilon_e + \varepsilon_p \tag{1}$$

where ε is the total strain tensor, ε_e is the elastic strain tensor and ε_p is the viscoplastic strain tensor.

(b) *Anisothermal elastic law*

$$\varepsilon_e = \frac{1+\nu}{E(T)}\sigma - \frac{\nu}{E(T)} Tr(\sigma)\mathbf{I} + \alpha(T)(T-T_0)\mathbf{I} \tag{2}$$

where $E(T)$ is the elastic modulus, ν is the Poisson ratio, $\alpha(T)$ is the thermal expansion coefficient, T_0 is the reference temperature in °C, σ is the stress tensor, $\mathbf{I}$ denotes the unit tensor and $Tr(\sigma) = \sigma_{kk}$ in the Cartesian component notation.

(c) *Viscoplastic strain rate*

$$\left.\begin{aligned} \dot{\varepsilon}_p &= \frac{\partial \Omega}{\partial \sigma} = \frac{3}{2}\dot{p}\frac{\sigma' - \mathbf{X}'}{J(\sigma - \mathbf{X})} \\ \text{where} \quad \dot{p} &= \left\langle \frac{J(\sigma - \mathbf{X}) - R - k^*}{K^*} \right\rangle^{n^*} \end{aligned}\right\}. \tag{3}$$

The brackets are defined by $\langle w \rangle = wH(w)$. $H\langle w \rangle$ is the Heaviside function ($H(w) = 0$ if $w < 0$, $H(w) = 1$ if $w \geqslant 0$) and Ω is the viscoplastic potential. $J(\sigma - \mathbf{X})$ is defined by Von-Mises criterion:

$$J(\sigma - \mathbf{X}) = \left[\frac{3}{2}(\sigma' - \mathbf{X}') : (\sigma' - \mathbf{X}')\right]^{1/2} \tag{4}$$

where σ' and $\mathbf{x}'$ are, respectively, the deviatoric part of the stress tensor σ and of the kinematic hardening tensor $\mathbf{X}$, k^* is a material parameter (temperature dependent) corresponding to the initial size of the elastic domain. K^* is the viscoplastic resistance, n^* is the rate sensitivity coefficient and R is the isotropic internal stress or the drag stress.

Assuming viscoplastic incompressibility, we suppose the presence of an elastic domain in the stress space. Its evolution is described by:

$$f = J(\sigma - \mathbf{X}) - R - k^* \leqslant 0. \tag{5}$$

(*d*) *The non-linear kinematic hardening*

Widely used in France (Chaboche, 1977; Marquis, 1979), these kinematic equations were initially introduced by Armstrong and Frederick (1966). Non-linearities are given as a back stress term in the Prager's rule:

$$\dot{\mathbf{X}} = \frac{2}{3}a^* c^* \dot{\varepsilon}_p - c^* \mathbf{X} \dot{p}. \tag{6}$$

$\mathbf{X}$ is the kinematic internal stress tensor or back stress tensor, c^* is the kinematic parameter of the hardening and a^* is the stress saturation of the non-linear kinematic model. In practise, we use many kinematic variables (Chaboche and Rousselier, 1983). For our study we have chosen two variables:

$$\mathbf{X} = \sum_i \mathbf{X}_i ; \dot{\mathbf{X}}_i = \frac{2}{3} a_i^* c_i^* \dot{\boldsymbol{\varepsilon}}_p - c_i^* \mathbf{X}_i \dot{p} \quad (i = 1, 2). \tag{7}$$

(*e*) *Plastic strain range memorization and isotropic hardening*

That internal variables keep a memory of the prior maximum plastic strain range was proposed by Chaboche *et al.* (1979). The general formulation consists of introducing a non-hardening surface in the plastic strain space. The evolution of this surface is described by:

$$F = \frac{2}{3} J\left(\boldsymbol{\varepsilon}_p - \boldsymbol{\xi}\right) - q \leqslant 0. \tag{8}$$

where q and $\boldsymbol{\xi}$ are, respectively, the radius and the center of this surface. Note that evolution of the non-hardening domain is allowed only when $F = 0$.

The selected evolution rule for q and $\boldsymbol{\xi}$ is defined by:

$$\dot{q} = \eta^* H(F) \langle \mathbf{n} : \mathbf{n}_1 \rangle \dot{p} ; \mathbf{n} = \sqrt{\frac{3}{2}} \frac{\boldsymbol{\sigma}' - \mathbf{X}'}{J(\boldsymbol{\sigma} - \mathbf{X})}$$

$$\mathbf{n}_1 = \sqrt{\frac{3}{2}} \frac{\boldsymbol{\varepsilon}_p - \boldsymbol{\xi}}{J(\boldsymbol{\varepsilon}_p - \boldsymbol{\xi})} ; \dot{\boldsymbol{\xi}} = \sqrt{\frac{3}{2}} (1 - \eta^*) H(F) \langle \mathbf{n} : \mathbf{n}_1 \rangle \mathbf{n}_1 \dot{p}. \tag{9}$$

In eqn (9) $\mathbf{n}$ and $\mathbf{n}_1$ are, respectively, the unit normals to the yield surface ($f = 0$) and to the memory surface ($F = 0$) and η^* is a memory plastic strain parameter, introduced by Ohno (1982) in order to allow a progressive memorization.

The isotropic hardening corresponds to slow changes during plastic flow. Its main role is to describe the cyclic softening. The simple isotropic rule can be written as:

$$dR = b^*(Q^* - R)\dot{p} \quad \text{with } R(0) = 0 \tag{10}$$

where b^* and Q^* are two additional parameters. Q^* is the value of R at stabilization state and b^* is associated with the saturation rate of this variable R.

For a better description of the cyclic softening observed in the experimental tests, two isotropic variables are introduced; one annoted R_2 for the fast decrease of stress in the first cycles, another variables annoted R_1 describing the slow evolution of stress during cycling until steady-state is reached. The variables R_1 and R_2 are defined by:

$$\dot{R}_1 = b^*(Q - R_1)\dot{p} ; \dot{R}_2 = bst^*(Qst^* - R_2)\dot{p} ; R = R_1 + R_2 \tag{11}$$

In eqn (11), Qst^* represents the value of R_2 in the stabilized state and bst^* represents the stabilization curve steepness for the isotropic hardening R_2.

The strain memory effect has been introduced by means of an additional internal variable which keeps a memory of the largest plastic strain range. The asymptotic isotropic state Q in eqn (11) will, therefore, be:

$$\dot{Q} = 2m^*(Q_M^* - Q)\dot{q} \tag{12}$$

q is the internal variable corresponding to the radius of the memory surface F (see eqn (8)).

Under tensile–compressive cycling, $q = (\Delta\varepsilon_{p\max})/2$, being the maximum plastic strain range. Q_M^* and m^* are material and temperature dependent parameters. Relation (12) is integrated and the saturation value of the hardening variable R_1 becomes:

$$Q = Q_M^* \cdot (1 - \exp(-m^* \cdot \Delta\varepsilon_p)). \tag{13}$$

The use of this model (eqns (1)–(13)) needs the determination of the parameters n^*, k^*, K^*, a_1^*, c_1^*, a_2^*, c_2^*, b^*, Qst^*, bst^*, η^*, m^* and Q_M^* which depend on material and temperature. These parameters must minimize the error between experimental curves and numerical curves deduced from the model.

3. ON THE PARAMETERS IDENTIFICATION PROCEDURE

The material used in the brake disc is the 28CrMoV5-8 steel. On the basis of experimental results (Samrout, 1996), cylindrical samples were submitted to uniaxial cyclic loadings (under tensile-compressive loadings) for several strain ranges $1\% \leqslant \Delta\varepsilon \leqslant 1.8\%$ at different temperatures $20°C \leqslant T \leqslant 600°C$ (the application of the brake pads leads to temperatures less than 600°C).

In opposite to the three-axial loadings which are difficult to control, the uniaxial cyclic loadings allow determining all the model parameters and are easy to achieve and to explain.

The model deduced from the uniaxial test is sufficient for a good reproduction of the real three-dimensional behavior of the material (Chaboche, 1986; Ben Cheikh, 1987). On the basis of the experimental results, a cyclic softening is observed.

In order to identify the set of parameters at each temperature, we had to perform:

- monotonic relaxation tests;
- cyclic tests run at several imposed strain ranges without holding time until rupture.

The AGICE program (automatic-graphic identification of constitutive equations) has a least squares method for the optimization of different parameters using the experimental results. Figure 1 shows the procedure used for the identification.

Table 1 gives the different parameters at 300°C. We made the same tests at 20, 200, 500 and 600°C. The unit of material parameters k^*, a_1^*, a_2^*, Q_M^*, Qst^* is MPa, the unit of K^* is MPa.s^{-1}, all others are dimensionless. For every temperature we have a set of values for the parameters, we use the least squares method to find a function which presents the required fit. The continuous function gives the parameter evolution vs temperature varying between 20 and 600°C.

For example, Figs 2–3 give the functions used, respectively, for the Young modulus E and the memory parameters m^*. The Young modulus E decreases with rising temperature. Its interpolation needs a simple exponential function (Fig. 2) in the form of:

$$E(T) = \delta + \beta(1 - e^{\chi T}) \tag{14}$$

with $\delta = 187.3$ GPa, $\beta = 14.7$ GPa and $\chi = 24.10^{-4}$°C. The other parameter is a decreasing and increasing function and needs a complex interpolation (Fig. 3).

4. FINITE ELEMENT SIMULATION AND VALIDATION OF THE ANISOTHERMAL MODEL

4.1. *Introduction of the obtained constitutive equations into a finite element program*

This section presents simulations of cyclic behavior of 28CrMoV5-8 steel in different strain ranges. All the parameters of this three-dimensional model were introduced into a finite element program Castem 2000. We utilized a cylindrical sample which was submitted to uniaxial loadings. For numerical simulations, an axisymmetric version of this sample was used. Only one finite element was used for the simulation. This element, in the middle of the sample, was submitted to an imposed strain. If $\Delta\sigma = \sigma_{maxi} - \sigma_{mini}$, Fig. 4 gives a comparison between experimental data and finite element modelling for the strain range $\Delta\varepsilon = 1.4\%$ when the temperature is at 20°C.

Figure 5 gives the simulation curve for the relaxation test at the same temperature. Figure 6 shows the stabilized curve (σ-ε) for $\Delta\varepsilon = 1.4\%$ at 20°C. In all cases, we have good agreement between the experimental data and the finite element modelling deduced from

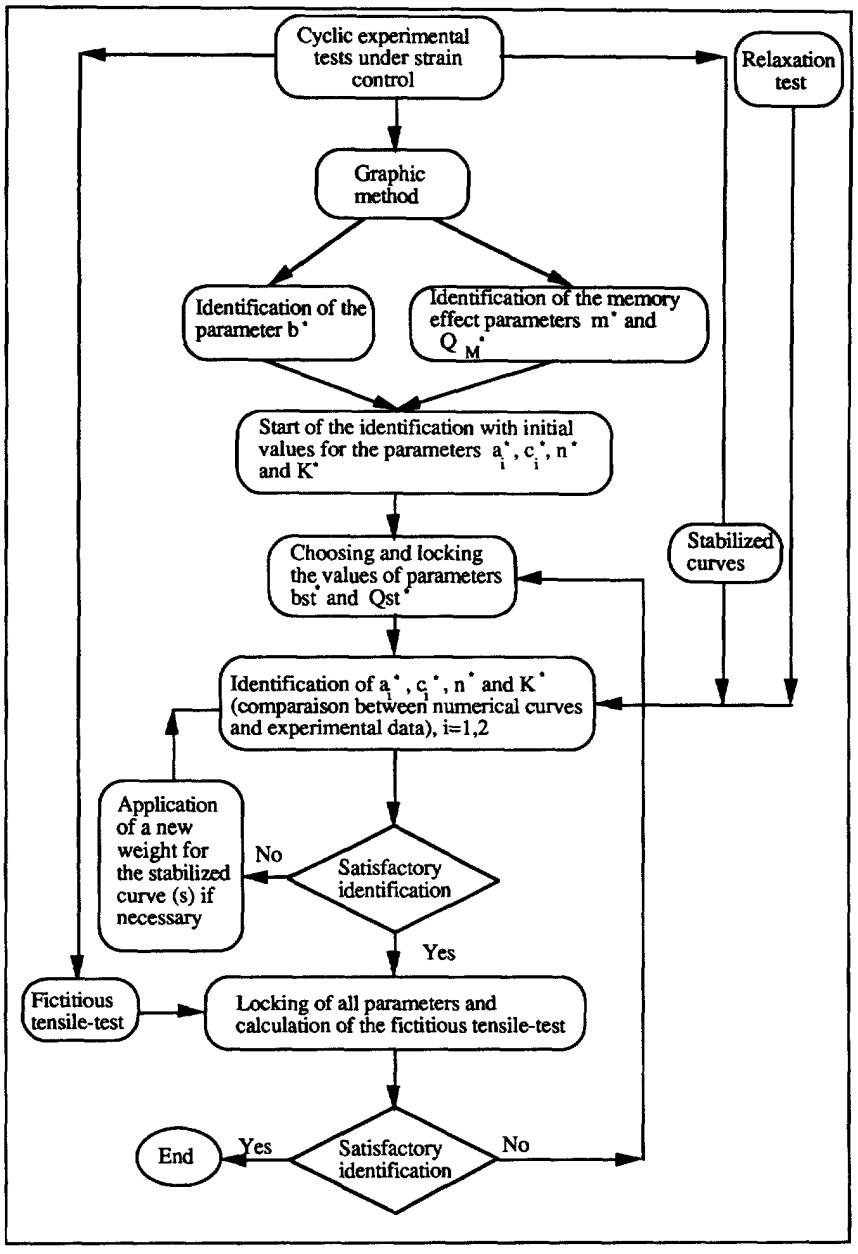

Fig. 1. Flow chart for the parameter identification.

Table 1. Material parameters for 28CrMoV5-8 steel at 300°C

k^*	a_1^*	c_1^*	a_2^*	c_2^*	b^*	bst^*	Qst^*	η^*	m^*	Q_M^*	n^*	K^*
201	272	2378	276	221	1.8	20	−40	0.2	338	−131	17	528

the proposed constitutive model. If we use only one isotropic variable (as in eqn (10)), we cannot have a valid numerical curve (Fig. 7). A second isotropic hardening variable allows us to improve the numerical curve, especially during the first few cycles.

4.2. *Validation of the anisothermal model*

A series of experimental tests under a temperature cycled between 200 and 600°C was undertaken. We analysed the thermomechanical cyclic loadings as shown in Figs 8 and 9.

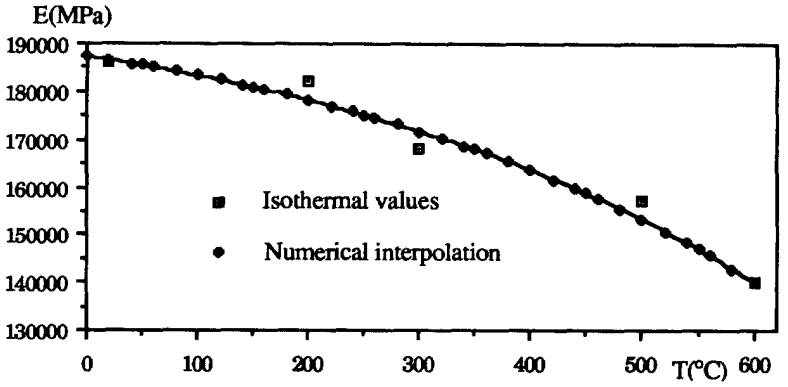

Fig. 2. Young's modulus versus temperature.

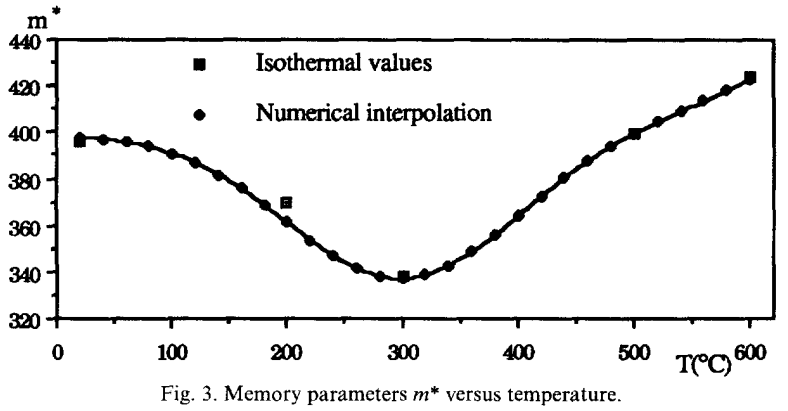

Fig. 3. Memory parameters m^* versus temperature.

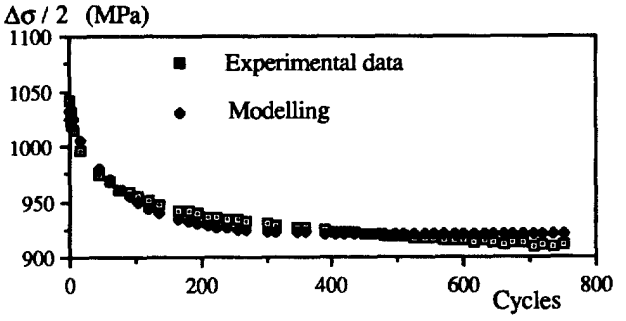

Fig. 4. Comparison between experimental curve and finite element simulation for $\Delta\varepsilon = 1.4\%$ at 20°C.

In Fig. 8, the temperature is cycled between 200 and 600°C under conditions of $\Delta\varepsilon = 1.4\%$. The cyclic thermal loading and applied strain are in-phase.

Figure 9 shows another test where the strain is cycled between -0.8 and 0.8% and the first thermal cycle begins at 200°C. Figures 10 and 11 give a comparison between numerical and experimental results, respectively, for the first cycle, and for the stabilized cycle when $\Delta\varepsilon = 1.4\%$. Figures 12 and 13 give the same comparison when $\Delta\varepsilon = 1.6\%$.

The stabilization of stress occurs rapidly (after approximately 12 cycles). The introduced anisothermal model leads to a good agreement between numerical results and experimental behavior. In the vicinity of 200°C, we observed an increasing effect of plasticity due to a temperature delay when decreasing the strain (the experimental temperature is not exactly in-phase with the strain after the first cycle).

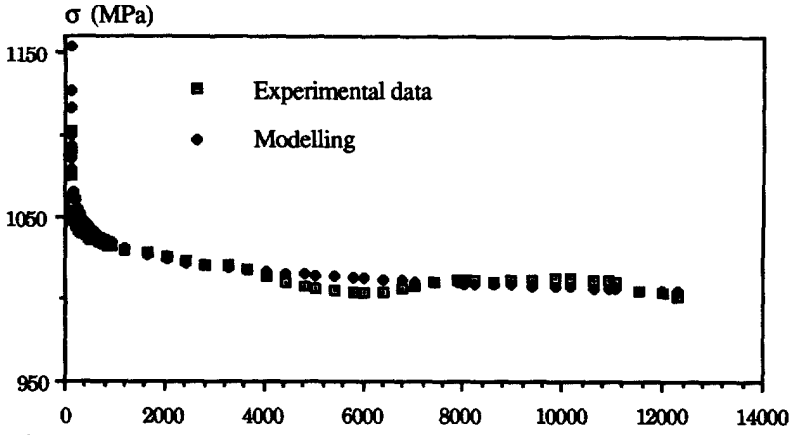

Fig. 5. Comparison between experimental data and numerical curve of the relaxation test at 20°C ($\varepsilon = 4\%$).

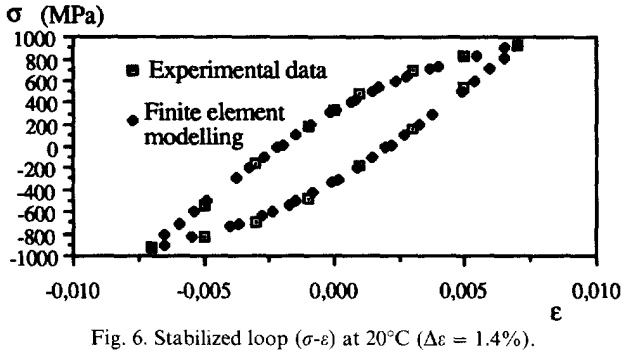

Fig. 6. Stabilized loop (σ-ε) at 20°C ($\Delta\varepsilon = 1.4\%$).

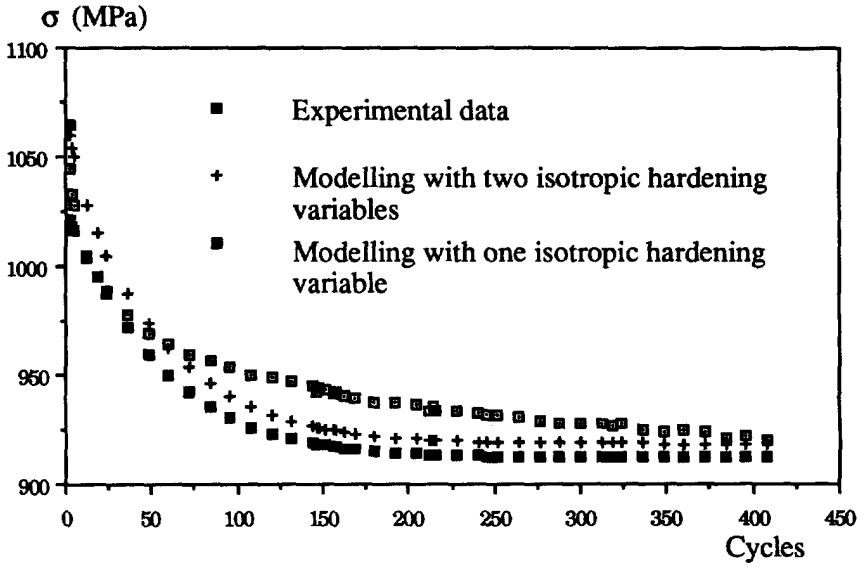

Fig. 7. Comparison of results with two and one isotropic hardening variable ($\Delta\varepsilon = 1.6\%$).

5. CONCLUSION

This paper presents an anisothermal elastoviscoplastic three-dimensional model for the description of behavior of a steel such as 28CrMoV5-8 used in the brake discs of a high speed train. The emphasis is put on the incorporation of strain memory terms and the use of two isotropic hardening variables. No mention is made of the difficulties in choosing the initial values needed for the determination of all parameter, (see Fig. 1). The numerical

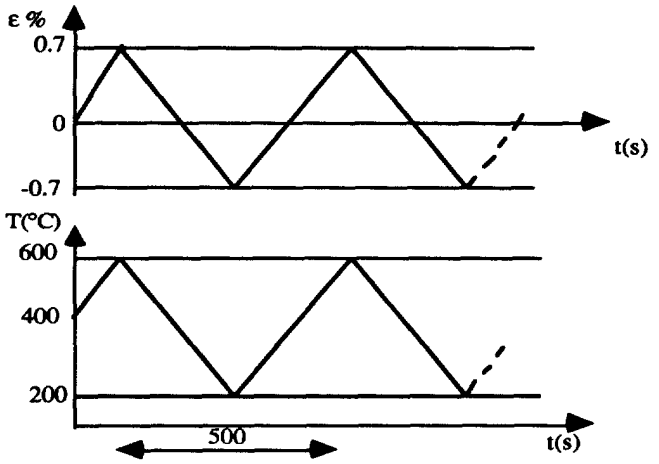

Fig. 8. Cyclical anisothermal test for $\Delta\varepsilon = 1.4\%$.

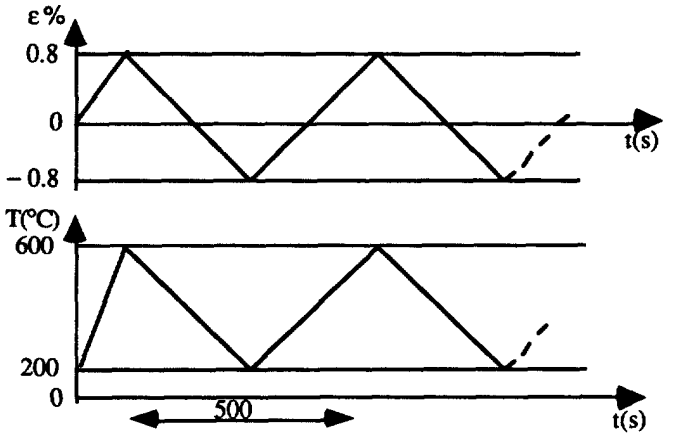

Fig. 9. Cyclical anisothermal test for $\Delta\varepsilon = 1.6\%$.

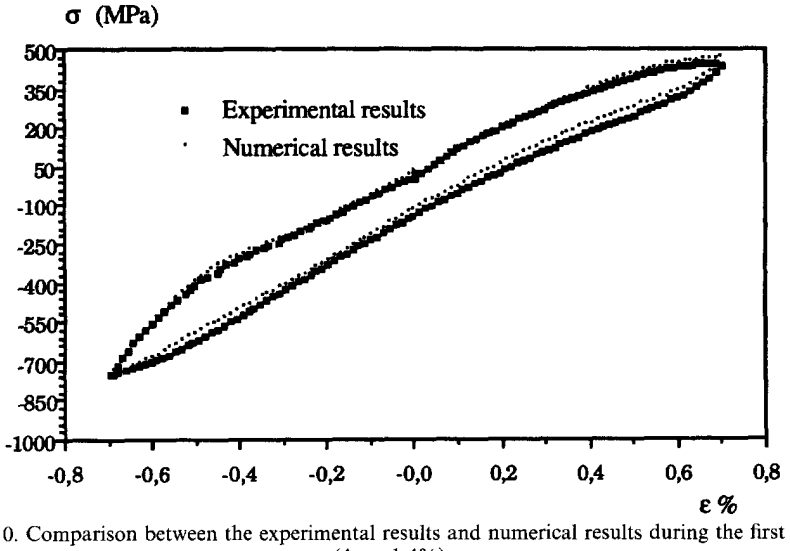

Fig. 10. Comparison between the experimental results and numerical results during the first cycle ($\Delta\varepsilon = 1.4\%$).

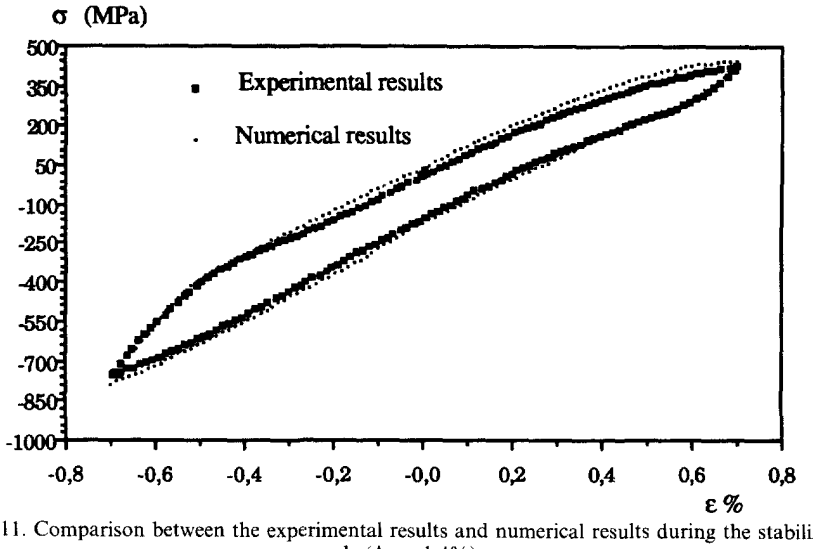

Fig. 11. Comparison between the experimental results and numerical results during the stabilized cycle ($\Delta\varepsilon = 1.4\%$).

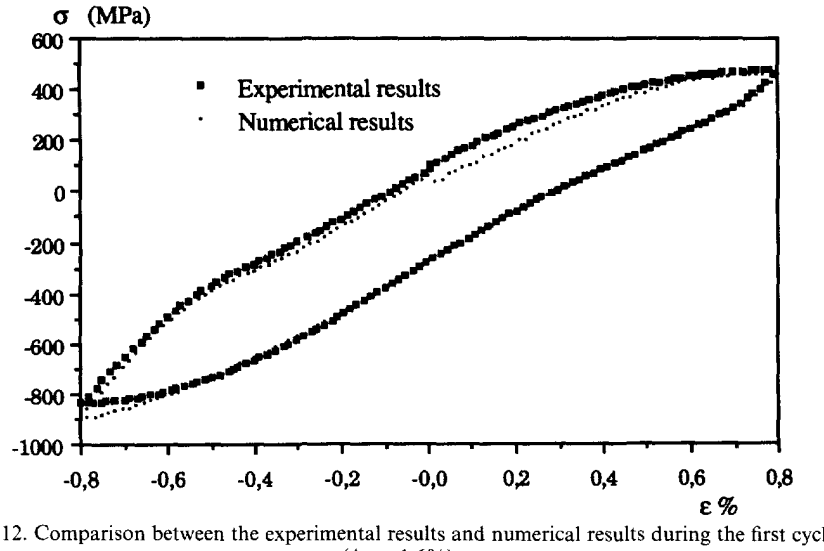

Fig. 12. Comparison between the experimental results and numerical results during the first cycles ($\Delta\varepsilon = 1.6\%$).

method introduced in the software AGICE is based on an integration complex scheme for the resolution of the implicit differential equations. The determination of the various parameters is based on the experimental results which include some measurement errors. There is no uniqueness of the values of material parameters. However, the obtained parameters approach as well as can be expected, those in the experimental curves. These parameters have a stationary aspect: a small perturbation does not alter the final results.

Using the parameter values obtained for each temperature, we give an anisothermal elastoviscoplastic model within the temperature range of 20–600°C. Experimental tests validate the proposed anisothermal model. A metallurgical analysis shows no structural transformation in the material up to 600°C.

Under a complex and repeated loading from the pressure of the brake pads on the friction surface, the brake disc suffers damage. In addition, we must determine the friction effects and the exchange coefficients between the brake disc and the brake pads. Before a good numerical modelization of the brake disc is achieved, we must therefore couple the proposed anisothermal model with a damage law and also introduce suitable exchange coefficients. For a complex stress analysis of the brake disc, we must also determine the

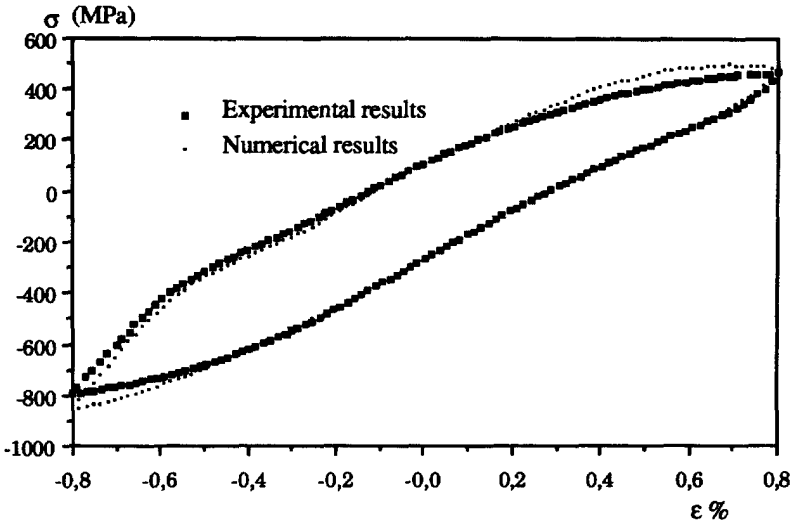

Fig. 13. Comparison between the experimental results and numerical results during the stabilized cycle ($\Delta\varepsilon = 1.6\%$).

anisothermal model of the brake pads which are of an organic material. Numerical boundary conditions need experimental data as the measuring of the temperature on the friction area which will be soon obtained from the test bench. This is what we shall do in our subsequent work.

REFERENCES

Armstrong, P. J. and Frederick, C. O. (1966) A mathematical representation of the multiaxial Bauschinger effect, G.E.G.B. Report RD/B/N 731.

Ben Cheikh, A. (1987) Elastoviscoplasticité à température variable. Thèse de Doctorat, Université de Paris-VI.

Chaboche, J. L. (1977) Viscoplastic constitutive equations for the description of cyclic and anisotropic behaviour of metals. *17th Polish Conference on Mechanics of Solids*, Szczyrk. Bul. de l'Acad. Polonaise des Sciences, Séries Sc. et Techn., 25, p. 33.

Chaboche, J. L. (1978) Description thermodynamique et phénoménologique de la viscoplasticité cyclique avec endommagement. Thèse de Doctorat d'Etat. Université Paris 6.

Chaboche, J. L. (1986) EVPCYCL: Un code d'éléments finis en viscoplasticité cyclique. La Recherche Aérospatiale, n° 2, Mars–Avril, pp. 91–112.

Chaboche, J. L. (1989) Lois de comportement en plasticité cyclique et en viscoplasticité cyclique. *International Journal of Plasticity*, **5**(3), 247–203.

Chaboche, J. L. and Rousselier, G. (1983) On the plastic and viscoplastic constitutive equations. Part I and II. *ASME Journal of Pressure Vessel Technology*, **105**, 153–164.

Chaboche, J. L., Dang Van and Cordier, G. (1979) *Proceedings of SMIRT 5 Division L.*, Berlin.

Chaboche, J. L., Nouailhas, D. et Savalle, S. (1991) AGICE: Logiciel pour l'identification interactive graphique des lois de comportement. La Recherche Aérospatiale. n° 3, Mai–Juin, pp. 59–76.

Kawai, M. and Ohashi, Y. (1987) Coupled effect between creep and plasticity of type 316 stainless steel at elevated temperature. *2nd International Conference on Constitutive Laws for Engineering Materials. Theory and Applications*, Tuscon, Arizona, eds, Desai *et al.* Elsevier, Oxford.

Krempl, E. and Yao, D. (1984) The viscoplasticity theory based on overstress applied to ratchetting and cyclic hardening. *2nd International Conference on Low-Cycle Fatique and Elasto-Plastic Behaviour of Materials*, Munich.

Marquis, D. (1979) Sur un modèle de plasticité rendant compte du comportement cyclique. *3ème Congrès Français de Mécanique*, Nancy.

Marquis, D. and Lemaitre, J. (1987) Modelling elasto-plasticity, damage and aging as coupled behaviour in engineering materials. *International Colloquium on Mechanisms and Mechanics of Plasticity*, Aussois, France.

Nouailhas, D. (1987) A viscoplastic modelling applied to stainless steel behaviour. *2nd International Conference on Constitutive Laws for Engineering Materials: Theory and Applications*, Tuscon, Arizona, eds Desai *et al.* Elsevier, Oxford.

Nouailhas, D. (1989) Unified modelling of cyclic viscoplasticity. Application to austenitic stainless steels. *International Journal of Plasticity*, **5**, 501–520.

Ohno, N. (1982) A constitutive model of cyclic plasticity with a non-hardening strain region. *Journal of Applied Mechanics*, **49**, 721.

Samrout, H., El Abdi, R., Levaillant, C. et Delagnes, D. (1996) Optimisation des paramètres de la loi de comportement d'un acier de disques de frein pour matérial ferroviaire. *First International Conference on Integrated Design and Manufacturing in Mechanical Engineering*, Nantes, Avril, pp. 937–946.

Tanaka, E., Murakami, S. and Ooka, M. (1987) Constitutive modelling of cyclic plasticity in non-proportional loading conditions. *2nd International Conference on Constitutive Laws for Engineering Materials: Theory and Applications*, Tuscon, eds, Desai *et al.* Elsevier, Oxford.